

Standing-wave acoustic trap for nonintrusive positioning of microparticles

Cite as: Journal of Applied Physics **78**, 4845 (1995); <https://doi.org/10.1063/1.359770>
Submitted: 17 April 1995 . Accepted: 29 June 1995 . Published Online: 17 August 1998

H. M. Hertz



View Online



Export Citation

ARTICLES YOU MAY BE INTERESTED IN

[TinyLev: A multi-emitter single-axis acoustic levitator](#)

Review of Scientific Instruments **88**, 085105 (2017); <https://doi.org/10.1063/1.4989995>

[Single beam acoustic trapping](#)

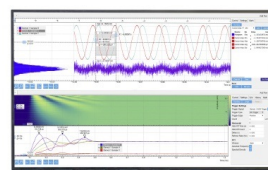
Applied Physics Letters **95**, 073701 (2009); <https://doi.org/10.1063/1.3206910>

[Independent trapping and manipulation of microparticles using dexterous acoustic tweezers](#)

Applied Physics Letters **104**, 154103 (2014); <https://doi.org/10.1063/1.4870489>

Challenge us.

What are your needs for periodic signal detection?



Zurich
Instruments

Standing-wave acoustic trap for nonintrusive positioning of microparticles

H. M. Hertz^{a)}

Department of Physics, Lund Institute of Technology, P.O. Box 118, S-221 00 Lund, Sweden

(Received 17 April 1995; accepted for publication 29 June 1995)

A nonintrusive three-dimensional trap for microscopic particles in a liquid is described. The trap is based on acoustic radiation forces in an ultrasonic confocal standing-wave cavity. Experiments at 11 MHz demonstrate the concept and verify the theoretically calculated forces. Theoretical calculations for higher-frequency systems indicate a significant potential for low-rms-displacement trapping of submicrometer particles, making the trap suitable for nonintrusive scanning near-field optical microscopy. © 1995 American Institute of Physics.

I. INTRODUCTION

Nonintrusive manipulation of microscopic particles using, e.g., single-beam optical traps, have important applications in biological and physical research. However, in many applications the optical trapping beam perturbs the studied object making traps based on alternative methods useful. In the present article the properties of an ultrasonic confocal standing-wave cavity for three-dimensional nonintrusive trapping and manipulation is investigated.

Macroscopic particles may be nonintrusively positioned and manipulated by several methods.¹ For microscopic particles "optical tweezers," or more correctly the single-beam gradient force optical trap,² has proven of great value for physical and biological research. Particles are trapped close to the focus of strongly focused laser beam as a result of the scattering and gradient forces due to optical radiation pressure. Using this trap, dielectric particles in the size range from tens of nanometers to tens of micrometers have been trapped. Furthermore, the trapping and manipulation of live viruses, cells, and subcellular organisms have been demonstrated,^{3,4} yielding information on, e.g., cell motility.⁵

We use the optical trap to nonintrusively position a 50–100 nm particle which acts as the microscopic light source in a new type of scanning near-field optical microscope.⁶ Near-field microscopes⁷ have obtained an order-of-magnitude better resolution than the conventional diffraction limit by scanning a microscopic light source in close proximity to the studied object. However, the positioning of the microscopic probe requires mechanical access to the studied object making studies of, e.g., biological object with rough surfaces or intervening membranes difficult. Using a nonintrusively positioned probe, such as the optically trapped microscopic light source, eliminates this restriction. Here the scattered or frequency-doubled light from the spatially well-defined trapped particle is used for the scanning microscopy. However, the optical trap requires transparent particles for the trapping, reducing the choice of probe materials. Furthermore, the maximum optical trapping power, and thus the forces on the trapped particle, are limited by the optical damage threshold of the studied object. For biological samples this threshold is approximately 100 mW of IR laser power.⁸ Finally, should the studied object have significant optical ab-

sorption at the wavelength of the trapping laser beam, thermally induced turbulence makes the trapping unstable resulting in loss of the particle. Thus, it would be favorable to trap the microscopic light source by a nonoptical process to extend the applicability of the method.

Although trapping with a single focused acoustic beam in principle is possible,⁹ standing-wave fields provide much larger trapping forces on microscopic particles. Standing acoustic waves have long been used to levitate and trap macroscopic objects. The theory of acoustic levitation and trapping is well understood.^{10,11} The method has been applied for studies of surface tension in mm-sized liquid drops,¹² shape oscillations and deformations in 100 μm droplets and biological cells,¹³ and mechanical properties of micron-sized biological material such as red blood cells.¹⁴ These experiments typically used a closed-cylinder levitation vial and frequencies from kHz up to a few 100 kHz.

In the present article an acoustic trap based on a standing-wave confocal ultrasonic cavity in liquid is described. By using focused transducers, micron-sized particles are three-dimensionally trapped in the velocity antinodes of the standing-wave acoustic field. We describe demonstration experiments at 11 MHz and compare the measured trapping forces with theory. Due to the large forces, this trap is an potential alternative to the optical trap used in nonintrusive scanned near-field optical microscopy if extended to higher acoustic frequencies.¹⁵ Furthermore, the acoustic standing-wave trap would allow absorbing objects such as fluorescent spheres to be used at probe particles, since the trapping and detection processes are decoupled.

II. THEORETICAL BACKGROUND

We consider here the forces of a standing-wave acoustic field on a rigid sphere. The derivations below follow Refs. 10 and 11. For a qualitative understanding it is useful to think of the acoustic radiation force as resulting from the gradient in an acoustic Bernoulli pressure. Thus, the sphere is trapped in the velocity antinodes of the standing-wave field. For an incompressible sphere considerably smaller than the acoustic wavelength, a more detailed analysis of the net acoustic trapping force F in the axial z direction of a standing-wave acoustic field results in¹⁰

$$F_z = V \left[B \left(\frac{\partial \bar{T}}{z} \right) - \left(\frac{\partial \bar{U}}{z} \right) \right]. \quad (1)$$

^{a)}Electronic mail: hertz@lucas.lu.se

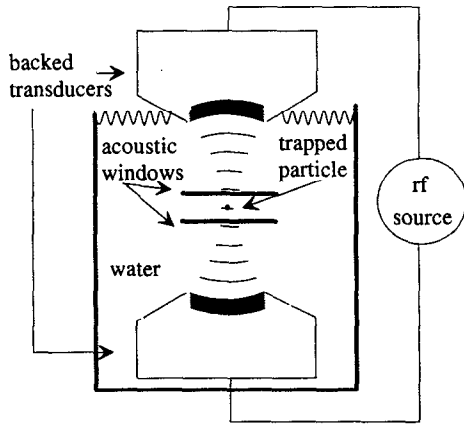


FIG. 1. Experimental arrangement for confocal standing-wave ultrasonic trapping of microscopic particles.

Here $B=3(\delta-1)/(2\delta+1)$, where $\delta=\rho/\rho_0$ and ρ and ρ_0 are the density of the sphere and the liquid, respectively, V is the particle volume, \bar{T} and \bar{U} are the second-order approximations to the time-averaged kinetic and potential energy densities, respectively. These energy densities may be written $T=\rho_0 u^2(z,t)/2$ and $U=p^2(z,t)/2\rho c_0^2$, where $u(z,t)$ is the particle velocity, $p(z,t)$ is the acoustic pressure, and c_0 is the speed of sound in the liquid. Thus, the force is proportional to the gradient of the intensity I_a of the acoustic beam via $I_a=p^2(z,t)/\rho_0 c_0$.

In the axial direction the acoustic pressure amplitude may be written $p(z,t)=P_a \cos(k_z z)\cos(\omega t)$. Here P_a is the peak acoustic pressure amplitude and k_z is the wave vector $2\pi/\lambda$, where λ is the acoustic wavelength. Thus, from Eq. (1) and following Ref. 10, the axial force F_z is

$$F_z = \frac{VP_a^2}{4\rho_0 c_0^2} \left(\frac{5\delta-2}{2\delta+1} \right) k_z \sin(2k_z z). \quad (2)$$

In the experiments described below we use a confocal ultrasonic cavity as outlined in Fig. 1. In order to evaluate the three-dimensional trapping stability, the acoustic forces in both the axial and the radial directions must be determined. In the radial direction in the focal plane we assume that

$$p(r,t) = P_a \frac{2J_1(Cr)}{Cr} \cos(\omega t),$$

due to plane-wave diffraction from a circular transducer. The constant C is determined experimentally from measurements of the Rayleigh range, i.e., the distance between the maximum and the first zero of $p(r,t)$. Thus, in analogy with the derivation of Eq. (2), the radial force F_r is given by

$$F_r = \frac{VP_a^2}{4\rho_0 c_0^2} \left(\frac{5\delta-2}{2\delta+1} \right) \frac{d}{dr} \left(\frac{2J_1(Cr)}{Cr} \right)^2. \quad (3)$$

The theoretical results are compared with experiments in the following section.

III. EXPERIMENTS

Figure 1 shows the experimental arrangement. Two lead-zirconate titanate focusing transducer bowls were mounted in a confocal arrangement in a water cell. For the 11 MHz experiments the transducer diameter and focusing radius were 10 and 22 mm, respectively. The distance between the transducers was 44 mm. Each transducer was backed with a damping material¹⁶ in order to suppress reflections. When the trap is in operation, the two transducers are parallel coupled and simultaneously driven by a rf amplifier resulting in a standing-wave pattern. The cavity is aligned by exciting only one transducer and maximizing the incident pressure amplitude on the other transducer.

In order to compare the experimental results with theory, the absolute acoustic pressure amplitude profile in the focal region must be known. The radial profile was determined by scanning a knife edge through the focus,¹⁷ yielding a Rayleigh range of $400 \pm 20 \mu\text{m}$. The knife-edge signal shape compared well with the assumption of a $J_1(Cr)/Cr$ radial profile, resulting in $C=0.0095 \mu\text{m}^{-1}$. The average acoustic pressure amplitude in the focal region was measured with a 1-mm-diam calibrated hydrophone¹⁶ with an absolute accuracy of $\pm 50\%$. The amplitude from the two focused transducers differed $\sim 5\%$. From these measurements the peak acoustic pressure amplitude and intensity of the standing-wave field in the focus of the confocal cavity was calculated.

Due to the slight difference in efficiency of the transducers, the two counterpropagating waves to do not form a perfect standing-wave acoustic field. Despite careful alignment a small residual propagating acoustic wave is present around the beam axis. Furthermore, small imperfections in the emitted acoustic spatial profiles result in low-intensity propagating acoustic waves outside the focal area. These propagating waves produce acoustic streaming, which obviously is detrimental when trapping microscopic objects. In principle, perfectly matched and identical transducers should eliminate this problem. The effect of the streaming on the trapped particles was practically eliminated by introducing two thin-film ($2 \mu\text{m}$) plastic windows at the focal region. The 5-mm-diam windows were separated by 1.5 mm. The attenuation by the windows was negligible.

The trapping was studied by dispersing glass spheres with a nominal average diameter of $2.1 \mu\text{m}$ (Duke Scientific Co.) in the water. Figure 2 shows a microscope photograph of the trapped particles around the focal region when illuminated by a HeNe laser. The acoustic windows have been removed for clarity. In order to obtain a clear photo, high particle concentration and a long accumulation time were used. This results in many particles in each trap. The distance between the traps is approximately $\sim 70 \mu\text{m}$ ($\lambda/2$). The flat structure of each band is due to the larger forces in the axial z direction than the radial direction (see below).

Measurements of the trapping force were performed by two methods: gravitational escape and viscous drag escape. In these experiments care was taken to inject only one particle in the central trap. A particle-water mixture is injected toward the central trap using a 0.5-mm-diam syringe directed toward the focus. With a reasonably high particle concentration in the injected fluid, the probability for trapping a par-



FIG. 2. Photograph of trapped particles in the standing-wave pattern.

ticle is high. Still the residual concentration of particles in the water cell is very low resulting in a small probability for collecting many particles in the trap during the experiment. Often, particles accumulate in more than one trap. Many of the traps may be emptied by lowering the acoustic power, thereby lowering the trapping force below the trapping threshold in the regions outside the focus.

In the first method, the trapping force in the vertical z direction was measured using gravitational escape. A particle was stably trapped at high acoustic power and then the power was lowered to allow escape of the particle due to gravitation. For the $2.1\text{ }\mu\text{m}$ particles, the gravitational escape occurs at $P_a = 0.045\text{ MPa}$ (corresponding to $\sim 0.07\text{ W/cm}^2$ total intensity), which corresponds to 0.09 pN according to Eq. (2). This compares well with the gravitational force on the particle, which is 0.07 pN , given the manufacturer's density data (2.42 g/cm^3) and compensating for the buoyancy due to the water. With $8\text{ }\mu\text{m}$ glass spheres the gravitational escape occurred at the same acoustic intensity. This is reasonable since both the gravitational force and the acoustic trapping force are proportional to the particle volume.

In the second method, a viscous drag force is applied to the particle by translating the water cell and the windows at constant speed relative to the transducers, thereby determining the radial forces. For this purpose the water cell was mounted on a smooth ball-bearing slide and coupled to a dc motor. The viscous drag force is assumed to be $F_{\text{visc}} = 6\eta av$, where η is the viscosity of water, a is the particle radius, and

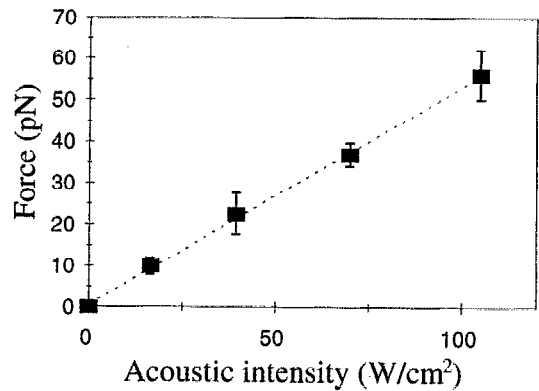


FIG. 3. Radial trapping force as a function acoustic intensity in an 11 MHz confocal standing-wave ultrasonic cavity.

v the speed. By increasing the speed until the particle escapes from the trap, the trapping force is determined. Figure 3 depicts the trapping force for the $2.1\text{-}\mu\text{m}$ -diam particles as a function of the acoustic intensity in the axial region of the standing-wave acoustic field. Each data point represents 3–5 measurements. The dashed line represents a linear regression fit to the data. The trapping force is clearly a linear function of the intensity and, thus, a linear function of the the square of the acoustic pressure amplitude as discussed in Sec. II. However, the theoretically calculated forces using Eq. (3) results in a factor 4 smaller forces than the experimentally determined forces. This is clearly a larger error than the $\pm 50\%$ accuracy in the acoustic pressure amplitude calibration would produce. Probably the discrepancy is due to the relatively wide size distribution of the glass spheres. Upon microscope inspection there are significant amounts of spheres with a diameter of $4\text{ }\mu\text{m}$ and a few with $5\text{ }\mu\text{m}$. Since the trapping force is proportional to particle volume, these larger spheres are more easily trapped and also require higher speed to be pulled out of the trap in the drag experiments. The theory agrees well with experiments if one assumes that $4\text{ }\mu\text{m}$ spheres are present in the trap. This is a reasonable explanation given the relatively high abundance of this size range.

In a final experiment to test alternative uses of the trap, red blood cells were stably trapped at peak pressures as low as 0.01 MPa . Clearly, these are not to be considered rigid nor spheres making comparison with theory difficult. However, the result indicates the possibility to manipulate biological objects much the same way as is done with the single-beam optical gradient force trap. As pointed out in Sec. I, acoustic manipulation may have distinctive advantages compared to optical, especially with respect to laser damage on materials which exhibit significant optical absorption.

IV. DISCUSSION

In this section the applicability of the acoustic trap for high-resolution trapped particle optical microscopy (TPOM)⁶ is discussed. This scanned near-field optical microscope (SNOM) allows nonintrusive studies of hitherto inaccessible objects as pointed out in Sec. I. Currently, our TPOM system is based on single optically trapped $50\text{--}100\text{ nm}$ particles.

Like in any SNOM, the resolution of the TPOM is determined by several factors, but is ultimately limited by the size of the microscopic probe which is scanned in close proximity to the studied object. In TPOM the effective size of the optical probe is its physical size convolved with its rms displacement in the trap due to Brownian motion. Below, the acoustical trap is compared to the optical with respect to resolution and other factors.

The particle's average position is determined by the velocity antinodes of the standing-wave field. Calculations of particle diffusion (Brownian motion) may be performed assuming that the acoustic trap is a harmonic potential well. For the small displacements ($< \lambda/10$) of interest in this study, the force in Eq. (1) is essentially a linear function of the displacement from the equilibrium position, making the assumption reasonable. For a one-dimensional harmonic potential well in the axial z direction, the rms displacement is¹⁸

$$\sqrt{\langle z^2 \rangle} = \sqrt{kT/M\omega^2}, \quad (4)$$

where k is the Boltzmann constant, T the temperature, and $M\omega^2$ the force constant of the harmonic oscillator. At the equilibrium position the force constant dF_z/dz is $2k_z F_{z,\max}$, where $F_{z,\max}$ is the maximum of F_z given by Eq. (2). For the radial r direction, the force constant dF_r/dr is calculated from Eq. (3).

Naturally, the current 11 MHz trap is not suitable for TPOM due to its large probe size ($\sim 2 \mu\text{m}$). Trapping smaller particles with low rms displacement requires higher force constants. This may be achieved by using GHz frequency transducers coupled to sapphire acoustic lenses. Such components are commercially available with, e.g., numerical aperture $\text{NA}=0.77$, for acoustic microscopy.¹⁹ Typically such transducers may produce an average acoustic intensity of 100 W/cm^2 without damaging living cells.²⁰ From Eqs. (2) and (4) it may be calculated that a confocal cavity of two such lenses separated, e.g., $80 \mu\text{m}$, and operated at 1 GHz with 1000 W/cm^2 (1:10 duty cycle) will result in a rms displacement in the z direction of $\sim 15 \text{ nm}$ for 60-nm-diameter glass particles. In the radial r direction the force constant for the $\text{NA}=0.77$ objective is smaller resulting in a rms displacement approximately twice that of the z direction. Higher acoustic intensities naturally produces smaller displacements.

The rms displacements calculated for the GHz ultrasonic trap compare favorably with similar calculations for the optical trap. In the optical trap the forces are determined by the scattering and gradient electromagnetic forces. As described in Ref. 6, optical trapping of a 60-nm-diam, $n \approx 2$ dielectric particle results in a rms displacement of 30–60 nm, assuming an optical power of 100 mW at $1.06 \mu\text{m}$ wavelength. The advantage of the ultrasonic trap may be even larger, since nonlinear effects in the focal region may result in even higher force constants due to sharper focusing of the harmonics.²¹

A potential problem with the high acoustic intensities is that turbulence is induced by acoustic streaming, resulting in instability of the trapping. Such turbulence was observed in the 11 MHz experiment above, and eliminated by introducing windows around the trapping region. However, in the

GHz case the small separation between the transducers and a sample holder positioned between the transducers (typically a few tens of μm distances) should help quench the turbulence. Assuming, for simplicity, that all the acoustic power is absorbed in the water between the acoustic lenses and that the emitted power from the two transducers is made equal within 0.1% and, the minimum turbulence length scale (Kolgomorov scale) is on the order of $10 \mu\text{m}$.²² Thus, the energy in eddies with smaller radii will be strongly reduced due to viscous losses while eddies with larger size scale are damped by the transducers and sample holders.

V. CONCLUSIONS

A confocal standing-wave ultrasonic trap suitable for high spatial resolution positioning of microscopic particles is described. In an 11 MHz demonstration experiment the theoretically calculated trapping forces are experimentally verified. Extending the results to GHz frequencies results in very small rms displacement trapping of nm-sized particles. Compared to the single-beam gradient force optical trap, the acoustic trap described here features smaller rms displacement due to Brownian motion. Furthermore, it extends the applicability of high-spatial-resolution trapping to new types of materials, e.g., absorbing or reflecting particles as compared to the optical trap, which generally requires transparent particles. When applied to nonintrusive near-field optical microscopy, the acoustic trap has the advantage over the optical trap that acoustic waves are used for the trapping and optical waves for the detection, thereby decoupling the trapping and detection system allowing a more flexible design of the microscope.

ACKNOWLEDGMENTS

The author gratefully acknowledges the help from Hans Persson with the transducer design, and valuable discussions with Thomas Hertz, Juergen Breiter-Hahn, Lars Malmqvist, Lars Rymell, and Magnus Berglund. This work was financed by the Swedish Natural Science Research Council, the Swedish Board for Industrial and Technical Development, the Carl Trygger Foundation, and the Crafoord Foundation.

¹E. H. Brandt, *Science* **243**, 349 (1989).

²A. Ashkin, J. M. Dziedzic, J. E. Bjorkholm, and S. Chu, *Opt. Lett.* **11**, 288 (1986).

³A. Ashkin and J. M. Dziedzic, *Science* **235**, 1517 (1987).

⁴W. H. Wright, G. J. Sonek, Y. Tadir, and M. W. Berns, *IEEE J. Quantum Electron.* **26**, 2148 (1990).

⁵A. Ashkin, K. Schütze, J. M. Dziedzic, U. Euteneuer, and M. Schliwa, *Nature* **348**, 346 (1990).

⁶L. Malmqvist and H. M. Hertz, *Opt. Commun.* **94**, 19 (1992); *Opt. Lett.* **19**, 853 (1994).

⁷E. Betzig and J. K. Trautman, *Science* **257**, 189 (1992).

⁸S. M. Block, in *Noninvasive Techniques in Cell Biology*, edited by J. K. Foskett and S. Grinstein (Wiley, New York, 1990), pp. 375–402.

⁹J. Wu and G. Du, *J. Acoust. Soc. Am.* **87**, 997 (1990); J. Wu, *ibid.* **89**, 2140 (1991).

¹⁰L. A. Crum, *J. Acoust. Soc. Am.* **50**, 157 (1971).

¹¹J. A. Rooney, in *Methods in Experimental Physics*, edited by P. D. Edmonds (Academic, New York, 1981), Vol. 19.

¹²E. H. Trinh, P. L. Marston, and J. L. Robey, *J. Coll. Interface Sci.* **124**, 95 (1988).

¹³Z. Zhu and R. E. Apfel, *J. Acoust. Soc. Am.* **78**, 1796 (1985).

- ¹⁴M. A. H. Weiser and R. E. Apfel, *J. Acoust. Soc. Am.* **71**, 1261 (1982).
- ¹⁵H. M. Hertz, L. Malmqvist, L. Rosengren, and K. Ljungberg, *Ultramicroscopy* **57**, 309 (1995).
- ¹⁶H. Persson, Department of Electrical Measurements, Lund Institute of Technology, P.O. Box 118, S-221 00 Lund, Sweden (personal communication, 1995).
- ¹⁷H. M. Hertz and R. L. Byer, *Opt. Lett.* **15**, 396 (1990).
- ¹⁸S. Chandrasekhar, *Rev. Mod. Phys.* **15**, 1 (1943).
- ¹⁹Leica GmbH, P.O. Box 2040, D-6330 Wetzlar, Germany.
- ²⁰A. Briggs, *Acoustic Microscopy* (Clarendon, Oxford, 1992), pp. 178–179.
- ²¹D. Rugar, *J. Appl. Phys.* **56**, 1338 (1984).
- ²²M. T. Landahl and E. Mollo-Christensen, *Turbulence and Random Processes in Fluid Mechanics* (Cambridge University Press, Cambridge, 1986), p. 10.